DNA-Bound Redox Activity of DNA Repair Glycosylases Containing [4Fe-4S] Clusters†

Amie K. Boal,‡ Eylon Yavin,‡ Olga A. Lukianova,§ Valerie L. O'Shea,§ Sheila S. David,*,§ and Jacqueline K. Barton*,‡

Division of Chemistry and Chemical Engineering, California Institute of Technology, Pasadena, California 91125, and Department of Chemistry, University of Utah, Salt Lake City, Utah 84112

Received November 29, 2004; Revised Manuscript Received April 8, 2005

ABSTRACT: MutY and endonuclease III, two DNA glycosylases from *Escherichia coli*, and AfUDG, a uracil DNA glycosylase from *Archeoglobus fulgidus*, are all base excision repair enzymes that contain the $[4Fe\text{-}4S]^{2+}$ cofactor. Here we demonstrate that, when bound to DNA, these repair enzymes become redox-active; binding to DNA shifts the redox potential of the $[4Fe\text{-}4S]^{3+/2+}$ couple to the range characteristic of high-potential iron proteins and activates the proteins toward oxidation. Electrochemistry on DNA-modified electrodes reveals potentials for Endo III and AfUDG of 58 and 95 mV versus NHE, respectively, comparable to 90 mV for MutY bound to DNA. In the absence of DNA modification of the electrode, no redox activity can be detected, and on electrodes modified with DNA containing an abasic site, the redox signals are dramatically attenuated; these observations show that the DNA base pair stack mediates electron transfer to the protein, and the potentials determined are for the *DNA-bound* protein. In EPR experiments at 10 K, redox activation upon DNA binding is also evident to yield the oxidized $[4Fe\text{-}4S]^{3+}$ cluster and the partially degraded $[3Fe\text{-}4S]^{1+}$ cluster. EPR signals at $g = 2.02$ and 1.99 for MutY and $g = 2.03$ and 2.01 for Endo III are seen upon oxidation of these proteins by $Co(phen)_3^{3+}$ in the presence of DNA and are characteristic of $[3Fe\text{-}4S]^{1+}$ clusters, while oxidation of AfUDG bound to DNA yields EPR signals at $g = 2.13$, 2.04, and 2.02, indicative of both $[4Fe\text{-}4S]^{3+}$ and $[3Fe\text{-}4S]^{1+}$ clusters. On the basis of this DNA-dependent redox activity, we propose a model for the rapid detection of DNA lesions using DNA-mediated electron transfer among these repair enzymes; redox activation upon DNA binding and charge transfer through well-matched DNA to an alternate bound repair protein can lead to the rapid redistribution of proteins onto genome sites in the vicinity of DNA lesions. This redox activation furthermore establishes a functional role for the ubiquitous [4Fe-4S] clusters in DNA repair enzymes that involves redox chemistry and provides a means to consider DNA-mediated signaling within the cell.

Encoded in the sequence of DNA is all of the genetic information of a cell. Yet the primary structure of DNA is remarkably dynamic (*1*). Large-scale rearrangements lead to gross changes in sequence, while chemical modifications to individual bases may lead to single base mutations. The consequences of large- and small-scale DNA sequence alterations can be beneficial, allowing for increased genetic diversity, but more often are deleterious, leading to mutation and disease. To counteract the harmful nature of DNA modification, organisms have developed diverse repair machinery aimed at protecting the genetic code (*2*).

Damage to a single DNA base is commonly repaired by two different pathways: direct damage reversal that repairs a damaged base without excising it and base excision repair (BER),[1] a pathway that removes a single damaged base and replaces it with a new one (*3*). The first step in the BER pathway involves the glycosylase enzyme, a protein that locates the damaged base and excises it from the helix. The excision reaction catalyzed by glycosylases is relatively well understood at the molecular level, but the mechanism by which these enzymes locate their substrates in the first place remains elusive (*4*). This detection challenge faced by glycosylases is formidable on two fronts. First, the base mismatches and modifications, the substrates for the glycosylases, often occur at low frequencies and are isolated among a vast amount of undamaged DNA (*1*). Second, the damage products detected by these enzymes represent very subtle deviations from the four natural DNA bases; often they vary by the addition or subtraction of a single functional group or even simply the mismatching of otherwise natural base pairs.

Some evidence suggests that glycosylases locate damage by processing along the DNA helix rather than randomly diffusing from site to site (*5*). Processive mechanisms offer

† Financial support for this work from the NIH (Grants GM49216 to J.K.B. and CA67985 to S.S.D.), the National Foundation for Cancer Research (J.K.B.), and the University of Utah Research Foundation (S.S.D.) is acknowledged.

* To whom correspondence should be addressed: e-mail, david@chem.utah.edu and jkbarton@caltech.edu; tel, 626-395-6075; fax, 626-577-4976.

‡ California Institute of Technology.

§ University of Utah.

[1] Abbreviations: MutY, *Escherichia coli* MutY; Endo III, *Escherichia coli* endonuclease III; AfUDG, *Archeoglobus fulgidus* uracil DNA glycosylase; MCH, mercaptohexanol; 8-oxoG, 7,8-dihydro-8-oxo-2′-deoxyguanosine; BER, base excision repair.

10.1021/bi047494n CCC: $30.25
Published on Web 05/18/2005

some enhancement in rate and efficiency by reducing the dimensionality of the search process. However, it is not clear that procession alone would be sufficient to account for the remarkable repair efficiency of these enzymes. In addition, BER enzymes operate in a complicated cellular environment, one in which a simple processive search process may be impossible (*6*). High salt concentrations exist that prevent electrostatic interactions between proteins and DNA (*7*). DNA is highly compact and covered in proteins much of the time, preventing rapid translocation along the helix (*8*). Glycosylases are often present in very low copy numbers (*9*) and may be involved in intricate relationships with other proteins including those related to other repair pathways, replication, and transcription processes (*10*−*17*). All of these facts indicate that damage detection by glycosylases is a highly complex process, one that may require more than one mechanism.

The base pair π-stack of double helical DNA has the unique ability to serve as a medium for charge transport over distances of at least 200 Å (*18*−*23*). This property of DNA is highly dependent on the integrity of the π-stack; perturbations that affect the structure and dynamics of DNA, including mismatched base pairs and damage products, greatly diminish the efficiency of DNA charge transport (*24*−*27*). In fact, devices based on DNA-mediated charge transport have proven to be powerful sensors of mutation in DNA (*28*). Additionally, evidence suggests that DNA charge transport can occur in biologically relevant environments: within a nucleosome core particle (*29*) and inside the nucleus of HeLa cells (*30*). While a biological role for DNA-mediated charge transport has not been definitively established, it has been proposed that DNA charge transport may be involved in DNA damage and repair (*31*−*33*). The exquisite sensitivity of DNA-mediated charge transport to perturbations in the π-stack prompts one to ask: might DNA repair enzymes exploit this property of DNA in their search for damage in the genome?

MutY, one of many glycosylases containing a [4Fe-4S] cluster (*34*−*37*), has recently displayed redox activity when investigated electrochemically on DNA-modified electrodes (*33*). MutY, containing 350 residues and the [4Fe-4S] cofactor, acts as a glycosylase to remove adenine from G·A and 7,8-dihydro-8-oxo-2′-deoxyguanonsine (8-oxo-G)·A mismatches (*38*−*52*). Initial characterization of the [4Fe-4S] cluster in MutY and endonuclease III (Endo III), a homologous enzyme with a substrate specificity instead for damaged pyrimidines (*53*−*62*), demonstrated that the cluster is in the 2+ oxidation state and is not readily oxidized or reduced within a physiologically relevant range of potentials; cluster decomposition occurs with oxidation, but photoreduction does yield the $[4Fe\text{-}4S]^{+}$ cluster (*34*). In the presence of DNA, however, MutY has a midpoint potential of +90 mV vs NHE (*33*). This redox potential is typical of high-potential iron proteins (*63*) indicating that, when MutY is bound to DNA, the redox potential of the enzyme shifts such that the 3+ oxidation state of the cluster becomes accessible. Earlier redox studies on MutY and Endo III conducted in the absence of DNA had argued for a structural rather than redox role for the ubiquitous cluster (*52*, *61*, *62*, *64*), yet some evidence had been obtained that the [4Fe-4S] cluster of MutY was not required for protein folding but was essential for activity (*65*).

Given the redox activity for MutY now demonstrated with DNA activation, a model has been proposed describing a role for the cluster in damage detection by MutY (*33*). In this model, DNA-mediated charge transport between two MutY proteins would serve as a fast, efficient scanning mechanism for damage in DNA; in the absence of intervening damage, DNA charge transport between proteins would be facile, permitting reduction with concomitant dissociation of the protein from undamaged regions of the genome. Through this fast scanning and sorting process, MutY would quickly concentrate near sites of damage in DNA. Local procession on a slower time scale to a nearby site would then allow for efficient substrate recognition and repair.

Endo III and *Archeoglobus fulgidus* UDG (AfUDG), like MutY, are glycosylases that contain a [4Fe-4S] cluster (*34*, *35*). Endo III repairs a wide variety of oxidized pyrimidines in DNA. The cluster in Endo III is well characterized spectroscopically (*34*, *64*). Endo III is of particular significance because, as with MutY, it is present in many organisms (*66*−*68*). AfUDG, on the other hand, is part of a special class of uracil glycosylases (*69*). These enzymes, known as family 4 UDGs, are present mostly in thermophilic bacteria and are the only family of UDGs to contain a [4Fe-4S] cluster (*35*, *69*−*74*). Cytosine deamination, the main process by which uracil is produced in DNA, is greatly enhanced at high temperatures (*75*). Despite this fact, thermophiles do not exhibit a higher mutation rate than other organisms (*76*). BER enzymes in thermophiles therefore face an even greater challenge in their quest to efficiently eliminate base damage. Perhaps the [4Fe-4S] cofactor in these enzymes is involved in enhancing the efficacy of repair?

Here we determine whether the DNA-bound redox activity seen with MutY is a more general characteristic of DNA glycosylases containing a [4Fe-4S] cluster. Endo III and AfUDG are both investigated electrochemically on DNA-modified electrodes to determine if the [4Fe-4S] cluster in each is redox-active and if that redox activity is DNA-mediated. Furthermore, all three proteins are examined by EPR spectroscopy with a Co(III) oxidant to establish whether DNA binding can also promote oxidation of the cluster in solution. These experiments have implications for the further development of our model to include the possibility of collaborative searching for damage by redox-active glycosylases.

EXPERIMENTAL PROCEDURES

Materials. All buffers were freshly prepared and filtered prior to use. Potassium ferricyanide was purchased from EM Science. Poly(dGC) ($\epsilon_{260} = 8400\ M^{-1}\ cm^{-1}$) was purchased from Amersham Pharmacia and was passed through spin columns (Bio-Rad) prior to use. All reagents for DNA synthesis were purchased from Glen Research.

$[Co(phen)_3]Cl_3$ was synthesized from $CoSO_4 \cdot 7H_2O$ according to a literature procedure (*77*). The cobalt complex was precipitated first as the PF_6 salt by adding a solution of NH_4PF_6 in water (20% w/v) to the reaction. The Co(III) complex was then converted to its chloride salt by dissolving 200 mg of $[Co(phen)_3](PF_6)_3$ in 5 mL of CH_3CN followed by the addition of $(tBu)_4NCl$ in 3 mL of CH_3CN (20% w/v) and formation of a yellow precipitate. After filtration and washing with acetonitrile, the isolated complex $[Co(phen)_3]Cl_3$ was fully characterized by NMR and mass spectrometry.

Protein Preparation. Endonuclease III was generously donated by Professor T. R. O'Connor (City of Hope) (*78*). The purification of AfUDG was modified from the reported procedure (*74*). The pET28a-*afung* plasmid containing the gene encoding the AfUDG protein was provided by Dr. William A. Franklin (Albert Einstein). Rosetta(DE3)pLysS cells (Novagen) transformed with the pET28a-*afung* plasmid were inoculated into LB media containing 34 μg/mL kanamycin and grown at 37 °C in 4 L to an $OD_{600} = 0.5-0.7$. At this stage, 1 mM isopropyl 1-thio-β-D-galactopyranoside (IPTG) was added, and the cells were incubated for an additional 6 h at 30 °C. The cells were harvested by centrifugation (10000 rpm, 7 min, 4 °C) and resuspended in 40 mL of ice-cold buffer L (25 mM Tris-HCl, 250 mM NaCl, pH 7.6) supplemented with 1 mM PMSF. The cells were disrupted by sonication (Branson Sonic Power Co., model 350, 70% pulse, 30 s on followed by 30 s off, repeated six times) and centrifuged to remove cellular debris (10000 rpm, 5 min, 4 °C). The proteins in the supernatant were batch-bound to Ni-NTA resin (1.5 mL/40 mL of supernatant) by gentle rocking at 4 °C for 1 h. The protein-bound resin was poured into an empty column (10 mL) and washed with 25 mL of 2× buffer L, followed by 5 mL of 1× buffer L. Protein was eluted with 2−5 mL of 1× buffer L containing 250 mM imidazole and diluted 8−10-fold with buffer A (25 mM Tris-HCl, pH 7.6). The protein solution was loaded onto a High S cartridge (Bio-Rad) and preequilibrated with 90% buffer A and 10% buffer B (25 mM Tris-HCl, pH 7.6, 1 M NaCl). The AfUDG protein was eluted by increasing the concentration of buffer B. Glycerol (10%) was added to the protein solution for storage at −80 °C. SDS−PAGE with Sypro Orange staining indicated the protein to be greater than 95% pure. Total protein concentrations were determined by the method of Bradford using BSA as the standard.

MutY was utilized in all experiments described here fused to maltose binding protein to allow experiments to be carried out at high concentrations. JM101 *muty*$^-$ *Escherichia coli* cells containing a pMAL-c2x-*muty* vector encoding maltose binding protein fused to the N-terminus of MutY were used to inoculate LB media (200 mL) containing 100 μg/mL ampicillin, 15 μg/mL tetracycline, and 0.02 g/mL glucose (LBATG). After overnight incubation at 37 °C, the culture was added to 4 L of LBATG which was further incubated with shaking at 37 °C until the OD at A_{600} was 0.6. IPTG (0.3 mM) was then added, and the cells were incubated at 30 °C for 3.5 h. After centrifugation (10000 rpm for 7 min), the cells were resuspended in 30 mL of 50 mM Tris-HCl, pH 8, containing 2 mM EDTA, 5% glycerol, 250 mM NaCl, 5 mM DTT, and 1 mM PMSF. The cells were lysed using a French press, the process being repeated twice, followed by centrifugation to remove cellular debris. The cell lysate (~40 mL) was loaded onto two separate 20 mL amylose (New England BioLabs) columns preequilibrated with buffer C (20 mM HEPES−KOH, pH 7.5 at 4 °C, 200 mM NaCl, 1 mM EDTA, and 1 mM DTT). MutY was eluted using 50 mL of buffer C containing 10 mM maltose. The protein-containing eluent was diluted 2-fold with buffer D (20 mM HEPES−KOH, pH 7.5 at 4 °C, 1 mM EDTA, 5% glycerol, and 1 mM DTT), filtered with a 0.45 μm filter, and loaded onto a 5 mL heparin column (Amersham Biosciences) on a Bio-Rad Bio-Logic. MutY was eluted using a gradient of 5−100% buffer D containing 1 M NaCl. Fractions containing pure MutY, as determined by SDS−PAGE with Sypro Orange staining, were concentrated, and the buffer was exchanged (20 mM sodium phosphate, pH 7.5, 100 mM NaCl, 10% glycerol, 1 mM EDTA) using an Amicon stirred ultrafiltration cell. The protein concentration was determined using an approximate ϵ(410 nm) of 17000 M^{-1} cm^{-1}.

Preparation of DNA-Modified Electrodes. Oligonucleotides were synthesized using standard phosphoramidite chemistry (*79*). Single strand oligonucleotides were modified at the 5′ end with a thiol moiety to facilitate covalent attachment to a gold electrode surface, as described earlier (*80*). Oligonucleotides were purified by HPLC, hybridized to their complements, and self-assembled into a loosely packed monolayer on a Au surface (*27*) in 50 mM NaCl and 5 mM sodium phosphate, pH 7.0. The electrode surface was then further passivated by incubation using mercaptohexanol (100 mM) in assembly buffer for 30 min. Electrodes were then rinsed with protein storage buffer (MutY and Endo III, 100 mM NaCl, 20 mM sodium phosphate, 1 mM EDTA, and 10% glycerol, pH 7.5; AfUDG, 25 mM Tris-HCl, 500 mM NaCl, and 5% glycerol, pH 7.6), and 50 μL of protein (550 μM MutY, 150 μM Endo III, or 360 μM AfUDG) in their storage buffers was added to the electrode surface and allowed to incubate for 10−15 min prior to measurement.

Electrochemistry Measurements. Low-volume constraints necessitated the use of a specialized low-volume cell for protein electrochemistry experiments. The working electrode consisted of a Au(111) on mica chip, and a Pt wire served as the auxiliary electrode. The reference electrode was a Ag/AgCl electrode modified with a tip containing 4% agarose in 3 M NaCl. This reference electrode was calibrated with ferrocene carboxylate and compared both to an unmodified Ag/AgCl reference electrode and to a saturated calomel electrode. All measurements were made using a BAS CV50W model electrochemical analyzer.

EPR Spectroscopy. X-band EPR spectra were obtained on a Bruker EMX spectrometer equipped with a rectangular cavity working in the TE_{102} mode. Low-temperature measurements (10 K) were conducted with an Oxford continuous-flow helium cryostat (temperature range 3.6−300 K). A frequency counter built into the microwave bridge provided accurate frequency values. Solutions were prepared by adding the protein (50 μM) to a solution of oxidant (150 μM) (with the exception of Endo III where the protein concentration was 10 μM and the oxidant concentration was 30 μM) in the presence or absence of poly(dGC) (1.5 mM in base pairs). Samples were incubated at ambient temperature (10 min) or heated to 55 °C (5 min) and cooled to ambient temperature. All samples were frozen in liquid nitrogen prior to EPR measurement at low temperature. EPR parameters were as follows: receiver gain = 5.64×10^3, modulation amplitude = 4 G, microwave power = 1.27 mW.

RESULTS

Electrochemistry on DNA-Modified Electrodes. The redox properties of each protein (MutY, Endo III, and AfUDG) were investigated on a loosely packed DNA-modified electrode surface passivated with mercaptohexanol (MCH) (Figure 1). AfUDG and Endo III both exhibit a redox signal using a DNA-modified electrode (Figure 2). The midpoint potential for AfUDG is 95 ± 3 mV versus NHE, while the

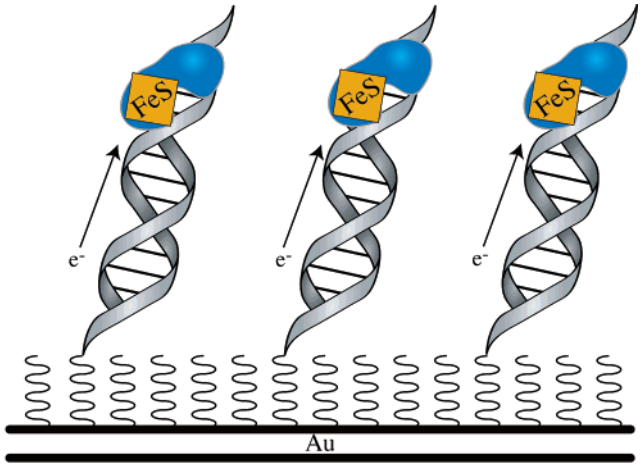

FIGURE 1: Schematic illustration of the electrochemical measurement of DNA-binding proteins containing [4Fe-4S] clusters at a DNA-modified Au electrode surface.

midpoint potential for Endo III is 58 ± 6 mV versus NHE. The measured midpoint potentials are similar to that previously measured for MutY of 90 mV versus NHE (*33*). The signals observed are reversible and robust over the course of the experiment. For each protein, the signal grows in over 5−10 min and remains at a constant intensity for up to 30 min after addition of the protein. No evidence of cluster degradation is observed during the experiment. Scan rate dependence measurements show a linear relationship between the peak current and the square root of the scan rate, an indication of a diffusion-limited process. However, measurements of electron transfer rates based on peak splitting (*81*) indicate a relatively slow rate of electron transfer (1−10 s^{-1}), consistent with earlier measurements of MutY (*33*). Importantly, as shown in Figure 2, each protein requires DNA for redox activity; at a MCH-modified surface lacking DNA, no signal is evident. In fact, even with 1 mM protein, no redox signal could be observed.

Covalent modification of electrodes is a technique commonly employed in protein electrochemistry both to concentrate proteins at the electrode surface and to properly orient buried redox centers for direct electron transfer with the electrode (*82*, *83*). To determine whether the redox activity observed here at a DNA-modified electrode is the result of direct interaction between the protein and the electrode surface or whether electron transfer to the cluster is mediated by the DNA π-stack, these proteins were investigated at a surface modified with a duplex containing an abasic site (thiol-modified strand SH-5′-AGTACAGT-CATCGCG hybridized to a complement containing an abasic site opposite the underlined thymine). We have determined previously that an intervening abasic site serves to diminish the redox signal from DNA-bound probes owing to the associated perturbation to the base pair stack (*28*). As evident in Figure 3, when each of these proteins is monitored electrochemically on a monolayer containing an abasic site, the redox signal is significantly attenuated. These observations support the idea that the redox chemistry obtained is DNA-mediated. The potential determined is therefore characteristic of the *DNA-bound* protein.

To test further that DNA binding promotes the shift in +3/+2 redox potential, activating the protein toward oxidation, we examined the protein electrochemistry on the DNA-modified surface before and after bulk electrolysis. Shown in Figure 4 are cyclic voltammograms for Endo III bound to the DNA-modified electrode before and after shifts in applied potential. As is evident, when the sample is equilibrated and then the potential is held at −350 mV for a discrete time interval so as to reduce the DNA-bound protein, the signal is attenuated, consistent with reduced protein dissociating from the DNA-modified electrode. Similarly, as is also shown in Figure 4, when the potential is held at +50 mV, to promote oxidation, the signal increases, consistent with protein oxidation yielding association with DNA. Calculation of net changes in area under the cyclic voltammograms reveals a 14% difference in both directions as a result of electrolysis. Analogous results were found with the other BER enzymes examined. While these results cannot provide a quantitative determination of solution binding affinities, these data nonetheless provide support for a greater DNA affinity for the protein in the oxidized form versus the reduced +2 state.

Low-Temperature EPR To Probe DNA-Bound Redox Chemistry. All three proteins were investigated by EPR spectroscopy in the presence and absence of DNA using $Co(phen)_3^{3+}$ as the oxidant. EPR measurements were performed at 10 K to observe any changes in the oxidation state of the [4Fe-4S] cluster. The [4Fe-4S] cluster in each of these proteins is in the 2+ oxidation state when free in solution, a configuration that is diamagnetic and EPR-silent (*34*, *35*, *84*). However, both the $[4Fe\text{-}4S]^{3+}$ and $[3Fe\text{-}4S]^{1+}$, a common damage product resulting from hydrolysis of the oxidized 4Fe-4S cluster (*63*, *85*, *86*), are EPR-active and give rise to distinctive spectra (*84*, *87*−*90*).

As expected, MutY, in the presence and absence of DNA, yields no EPR signal. The [4Fe-4S] cluster in MutY is largely in the 2+ oxidation state and EPR-silent. When MutY (50 μM) is incubated with $[Co(phen)_3]^{3+}$ (150 μM), a small signal appears that looks much like a $[3Fe\text{-}4S]^{+}$ cluster (*85*, *89*, *90*) with g values at 2.02 and 1.99 (Figure 5). In the presence of DNA and $[Co(phen)_3]^{3+}$ (150 μM), this signal is also evident but the intensity is much greater (∼4-fold by integration). It appears then that the presence of DNA enhances oxidation by Co(III). Since the cobalt complex binds DNA (*91*, *92*), albeit weakly, we also examined the oxidation reaction with an excess of $[Co(phen)_3]^{3+}$. Addition of 500 μM $[Co(phen)_3]^{3+}$ in the absence of DNA results only in a small increase in signal intensity; some interaction of the protein with the cobalt complex at these high concentrations is expected, yet without DNA little reaction occurs. These results are therefore also consistent with DNA binding serving to shift the oxidation potential of the cluster, activating the cluster toward oxidation.

Endo III also does not exhibit an EPR signal without oxidant in the presence or absence of DNA. Like MutY, upon addition of $[Co(phen)_3]^{3+}$ (30 μM) to Endo III (10 μM), a signal appears with g = 2.03 and 2.01, consistent with formation of a $[3Fe\text{-}4S]^{1+}$ cluster (Figure 6) (*89*, *90*). This signal also increases in intensity in the presence of DNA, although the enhancement is not as high as for MutY.

We also examined repair protein oxidation by ferricyanide in the presence and absence of DNA. A similar enhancement in cluster oxidation was observed in the presence of DNA (data not shown). However, ferricyanide is also known to promote oxidation of the cluster without DNA (*34*, *35*).

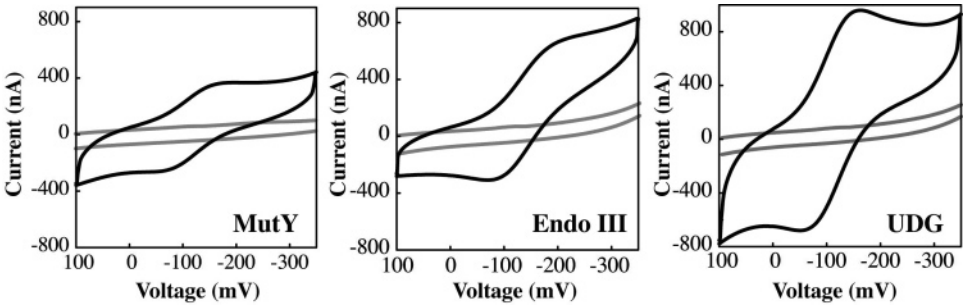

FIGURE 2: Cyclic voltammetry of MutY (left), Endo III (middle), and AfUDG (right) at DNA-modified electrodes (shown in black) (Ag/AgCl reference electrode, Pt auxiliary electrode, 50 mV/s scan rate). Buffer conditions for MutY and Endo III are 100 mM NaCl, 20 mM sodium phosphate, 1 mM EDTA, and 10% glycerol, pH 7.0. Buffer conditions for AfUDG are 25 mM Tris-HCl, 500 mM NaCl, and 5% glycerol, pH 7.6. Average potentials, based on several trials, are 90 mV for MutY, 59 mV for Endo III, and 95 mV for AfUDG, all versus NHE. DNA is required to observe the protein redox activity; proteins examined on a MCH-modified electrode (shown in gray) exhibit no electrochemical signal.

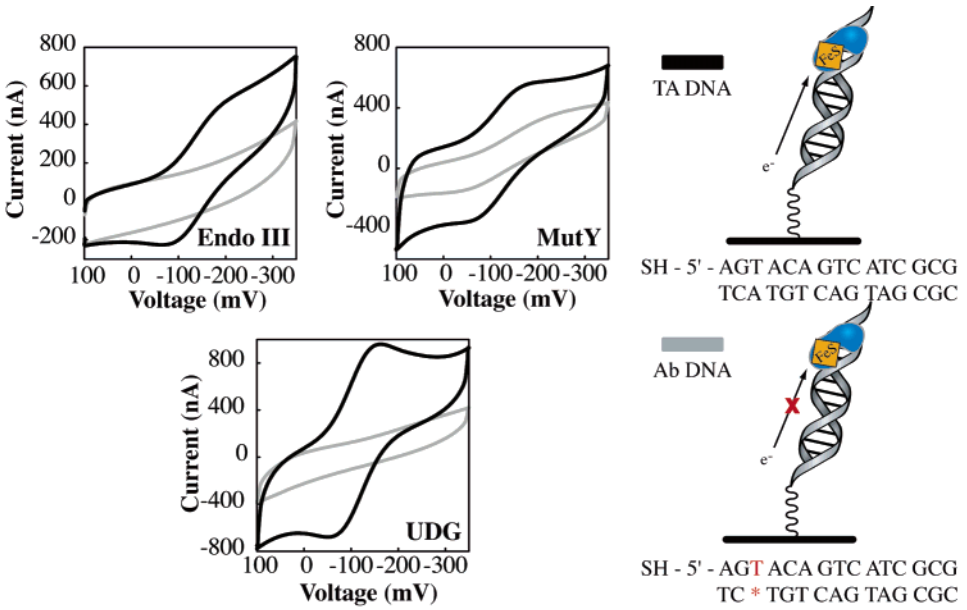

FIGURE 3: Electrochemistry (clockwise from top right) of MutY, AfUDG, and Endo III at an electrode modified with well-matched DNA duplexes (TA DNA in black) or DNA duplexes containing an abasic site (Ab DNA in gray) as measured by cyclic voltammetry (Ag/AgCl reference electrode, Pt auxiliary electrode, 50 mV/s scan rate). Buffer conditions for MutY and Endo III are 100 mM NaCl, 20 mM sodium phosphate, 1 mM EDTA, and 10% glycerol, pH 7.0. Buffer conditions for AfUDG are 25 mM Tris-HCl, 500 mM NaCl, and 5% glycerol, pH 7.6.

AfUDG in the presence or absence of DNA is EPR-silent as well. Unlike MutY and Endo III, AfUDG (50 μM) in the presence of $[Co(phen)_3]^{3+}$ (150 μM) is also EPR-silent in the absence of DNA. When DNA is included, however, a signal appears with g values at 2.13 and 2.04, typical of a $[4Fe\text{-}4S]^{3+}$ cluster (*87*, *88*) (Figure 7). Since AfUDG is isolated from a thermophilic organism, these samples were also investigated following incubation at 55 °C for 5 min. The same pattern is evident; AfUDG with DNA is EPR-silent as is AfUDG with $[Co(phen)_3]^{3+}$ while AfUDG with DNA and $[Co(phen)_3]^{3+}$ elicits a signal. However, this signal has a g value of 2.02, indicating that the cluster is likely in the $[3Fe\text{-}4S]^{1+}$ configuration. Previous studies examining oxidation of the cluster in family 4 UDG from *Pyrobaculum aerophilum* by ferricyanide demonstrated that a mixture of $[4Fe\text{-}4S]^{3+}$ and $[3Fe\text{-}4S]^{1+}$ species is formed in the absence of DNA (*35*). It is therefore apparent that this repair enzyme also is activated toward oxidation of its [4Fe-4S] cluster upon DNA binding.

DISCUSSION

Redox Activation of BER Enzymes upon DNA Binding. Electrochemical measurements of Endo III and AfUDG using DNA-modified electrodes demonstrate that, like MutY, both of these enzymes that contain a [4Fe-4S] cluster are redox-active when bound to DNA. Both BER enzymes show potentials on DNA-modified electrodes in the physiological range, with potentials of ~100 mV versus NHE, typical of high-potential iron proteins (*63*) and similar to MutY (*33*). Solution studies with mediators had shown that the proteins could not be easily oxidized in the absence of DNA, and estimates for the more accessible 2+/1+ couple were made of <-600 mV versus NHE (*34*). Without DNA attached to the gold electrodes, neither oxidation nor reduction of these proteins is observed here electrochemically. Thus protein binding to DNA appears to shift the redox potential, activating the $[4Fe\text{-}4S]^{2+}$ cluster toward oxidation.

Further support for this redox activation is apparent in monitoring changes in DNA-bound protein as a function of

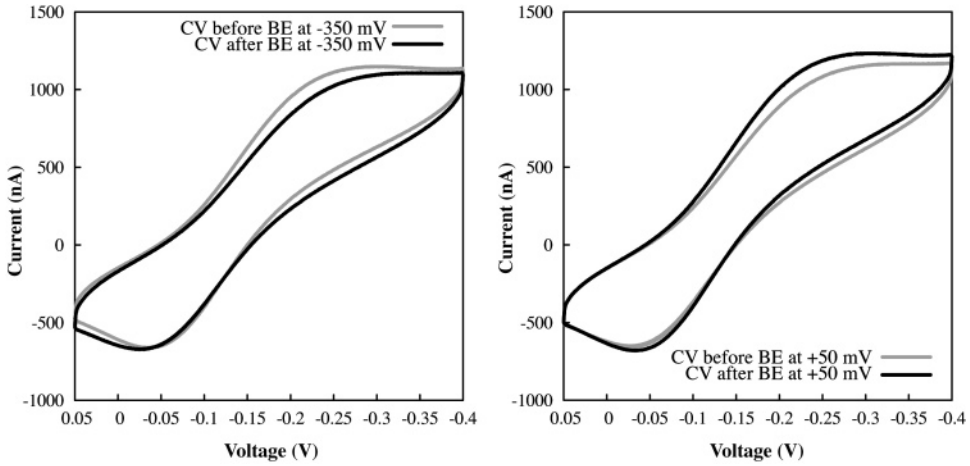

FIGURE 4: Cyclic voltammetry of endonuclease III before and after bulk electrolysis. The left panel shows CV before (gray trace) and after (black trace) bulk electrolysis for 5 min at −350 mV (versus Ag/AgCl). The right panel shows CV before (gray trace) and after (black trace) bulk electrolysis for 5 min at +50 mV (versus Ag/AgCl). An increase in peak intensity is evident after electrolysis at +50 mV, whereas a corresponding decrease is observed after electrolysis at −350 mV.

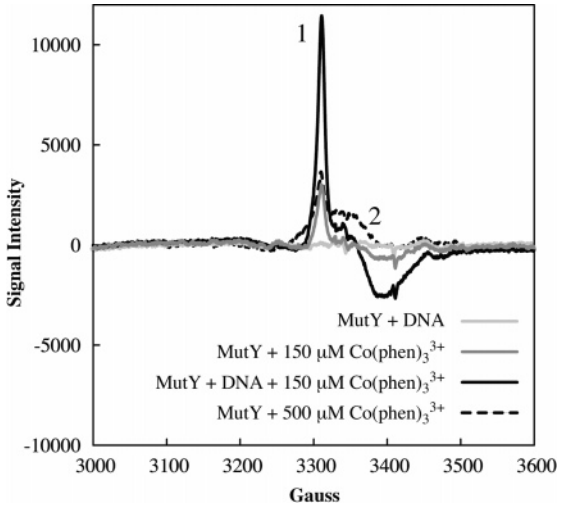

FIGURE 5: EPR spectroscopy at 10 K of MutY in the presence of DNA (light gray), 150 μM $[Co(phen)_3]^{3+}$ but no DNA (dark gray), 500 μM $[Co(phen)_3]^{3+}$ but no DNA (dotted line), and MutY with DNA and 150 μM Co(III) (black). Signal 1 shows $g = 2.02$; signal 2 shows $g = 1.99$.

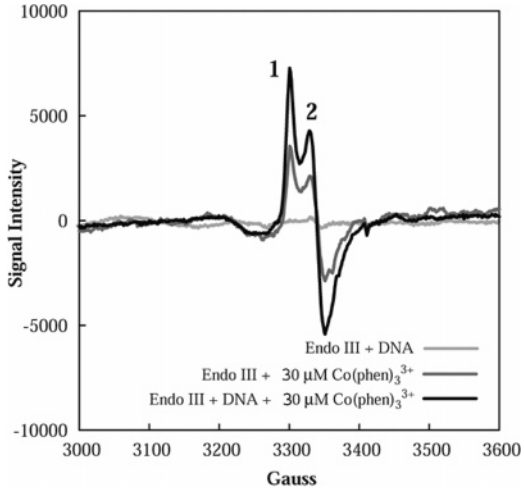

FIGURE 6: EPR spectroscopy at 10 K of Endo III in the presence of DNA (light gray), 30 μM $[Co(phen)_3]^{3+}$ but no DNA (dark gray), and with both DNA and 30 μM Co(III) (black). Signal 1 shows $g = 2.03$; signal 2 shows $g = 2.01$.

applied potential. When the DNA-modified electrodes are equilibrated with protein, but then the applied potential is shifted toward more negative potentials, reducing the protein, some protein dissociation from the electrode is evident. Similarly, shifting the potential to more positive values, to promote oxidation, increases the DNA-bound protein signal. While these data do not provide a quantitative measure of the difference in DNA-binding affinity with protein in the reduced versus oxidized form, these data do qualitatively support an increase in binding affinity for the protein with the [4Fe-4S] cluster in the +3 state versus the +2 state. In other words, thermodynamically, DNA binding activates the protein toward oxidation. A quantitative determination of this difference in binding affinity for the protein with cluster in the +3 versus +2 form may not be possible technically, since cluster oxidation in the absence of DNA clearly leads to cluster decomposition. On the DNA-modified electrodes, however, the redox cycle appears to be reversible.

That DNA binding would shift the potential is reasonable to expect. The redox potentials of $[4Fe\text{-}4S]^{2+}$ clusters are well known to vary considerably depending upon their environment (*63*, *93*). On the basis of crystal structures of MutY (*94*) and Endo III (*95*) bound to DNA, it is apparent that the iron−sulfur cluster is located near amino acid residues that contact DNA, so that DNA binding changes the environment for the cluster, taking it from an exposed and polar environment in the absence of DNA to a more hydrophobic environment in the presence of DNA. Moreover, the substrate binding affinity of MutY has been shown to be extremely sensitive to alterations of amino acids in the cluster coordination domain consistent with an intimate association of this region with DNA (*84*). It is reasonable to consider, then, that in the absence of DNA the [4Fe-4S] cluster is more ferredoxin-like, with the 2+/1+ couple being more accessible (*96*). Estimates for the reduction potential for the $[4Fe\text{-}4S]^{2+}$ cluster of Endo III of ∼−600 mV are consistent with this characterization. However, DNA binding may make the cluster environment more similar to high-potential iron proteins, with the 2+/3+ couple being more accessible in the physiological regime (*96*). Indeed, the DNA-bound potentials of 100 mV we observe are characteristic of high-potential iron proteins. Estimates based upon model

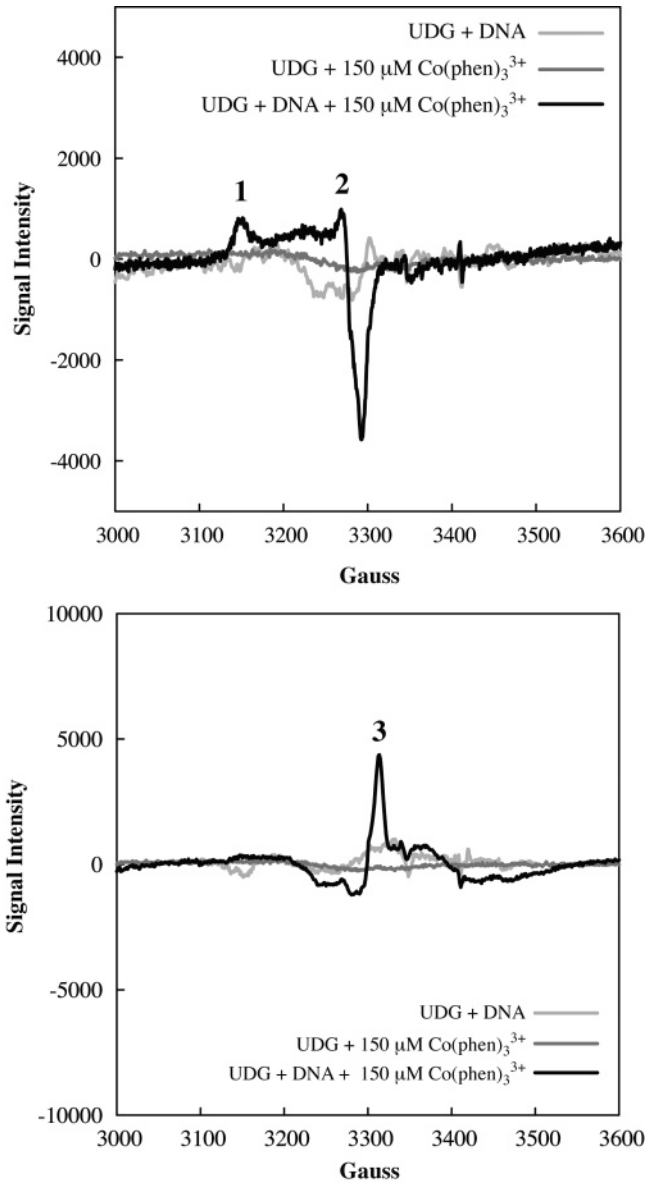

FIGURE 7: EPR spectroscopy at 10 K of AfUDG in the presence of DNA (light gray), 150 μM $[Co(phen)_3]^{3+}$ but no DNA (dark gray), and with both DNA and 150 μM Co(III) (black). Shown above after incubation at ambient temperature and below after incubation at 55 °C. Signal 1 shows $g = 2.13$; signal 2 shows $g = 2.04$; signal 3 shows $g = 2.02$.

studies for the difference in potential for the 3+/2+ couple versus the 2+/1+ couple are ≥1.0 V, both for ferredoxin-like clusters and for high-potential iron centers (*63*, *93*, *96*). Using a conservative value of 1.0 V for this difference, a value of −600 mV for the 2+/1+ cluster potential of Endo III without DNA, and the measured potential of 90 mV for the DNA-bound 3+/2+ couple suggests that DNA binding shifts the 3+/2+ potential 310 mV more negative. Thermodynamically, this 300 mV shift would correspond to a change in binding affinity between the +2 and +3 states of more than 4 orders of magnitude.

The EPR results also are consistent with DNA binding activating the cluster toward oxidation. While some oxidation by $Co(phen)_3^{3+}$ in the absence of DNA is found, significant enhancements in oxidation are apparent in the presence of DNA. Earlier results had shown some evidence of irreversible oxidation of Endo III by ferricyanide (*34*), but no enhancement with DNA binding was explored. Here it is noteworthy that $Co(phen)_3^{3+}$, an oxidant with potential similar to ferricyanide, binds to DNA (*91*, *92*). Hence the enhancement could reflect an increase in local concentration of the cobalt complex near the DNA-bound BER enzyme; 10 times higher concentrations of $Co(phen)_3^{3+}$ without DNA showed no increased oxidation, however. Alternatively, the oxidation of the protein by $Co(phen)_3^{3+}$ might be DNA-mediated. $Co(phen)_3^{3+}$ binds DNA by partial intercalation (*92*), facilitating coupling into the base pair stack to enable a DNA-mediated reaction.

Table 1: Comparison of EPR Data to Literature Values

protein	cluster type[a]	*g*-value[b]	lit. *g*-value	ref
MutY	$[3Fe\text{-}4S]^{1+}$	2.02, 1.99	2.02, 1.99[c]	*80*
Endo III	$[3Fe\text{-}4S]^{1+}$	2.03, 2.01	2.03, 2.01, 1.99[d]	*34*
AfUDG	$[3Fe\text{-}4S]^{1+}$	2.02	2.02[e]	*35*
	$[4Fe\text{-}4S]^{3+}$	2.13, 2.04	2.12, 2.04[e]	
R. globiformus HiPIP	$[4Fe\text{-}4S]^{3+}$		2.12, 2.03	*81*, *88*
E. halophila HiPIP			2.14, 2.03	
D. gigas FdII	$[3Fe\text{-}4S]^{1+}$		2.02, 2.00	*89*, *90*
beef heart aconitase			2.01	

[a] As observed by EPR spectroscopy at 10 K. [b] As measured in the presence of $Co(phen)_3^{3+}$ and DNA. [c] As measured for C199H MutY. [d] As measured for Endo III treated with ferricyanide. [e] As measured for AfUDG treated with ferricyanide.

The electrochemical results using DNA-modified electrodes show clearly that the charge transport reaction to oxidize the cluster can be DNA-mediated. With all of these proteins, incubation at a DNA-modified surface containing an abasic site yields a drastically attenuated signal compared to that found with a well-matched DNA duplex. This attenuation indicates that the DNA base pair stack must mediate electron transfer to the cluster rather than simply serving to locally concentrate the enzyme at the electrode. DNA-mediated charge transfer to the cluster requires an intact base pair π-stack.

Characteristics of the Oxidized Protein. EPR spectroscopy is used commonly to characterize [4Fe-4S] clusters and their oxidation states. Table 1 summarizes the results obtained here and comparisons to other results for different proteins containing [4Fe-4S] clusters. Based upon comparative *g* values, MutY, Endo III, and AfUDG, upon DNA binding in the presence of an oxidant, primarily promote formation of the $[3Fe\text{-}4S]^{1+}$ cluster. Some evidence for the directly oxidized cluster, $[4Fe\text{-}4S]^{3+}$, is also found, however, with AfUDG upon DNA binding.

High-potential iron proteins are known to be susceptible to degradation through reaction with water and oxygen (*63*):

$$[4Fe\text{-}4S]^{2+} \xleftrightarrow[\text{oxidant}]{\text{DNA}} [4Fe\text{-}4S]^{3+} \quad (1)$$

$$[4Fe\text{-}4S]^{3+} \xleftrightarrow{H_2O/O_2} [3Fe\text{-}4S]^{1+} \quad (2)$$

The $[4Fe\text{-}4S]^{3+}$ cluster can lose an iron to form the $[3Fe\text{-}4S]^{1+}$ cluster. This degradative process frequently occurs in [4Fe-4S] proteins as a result of oxidative damage (*85*). While the electrochemistry results indicate that DNA activates the $[4Fe\text{-}4S]^{2+}$ cluster toward oxidation in all three proteins and that oxidation can be reversed, MutY and Endo III only show a signal typical of a $[3Fe\text{-}4S]^{1+}$ cluster by EPR spectroscopy.

With MutY and Endo III, it is likely that the low temperature required to observe the cluster by EPR (10 K) destabilizes the protein such that the cluster falls apart; electrochemistry results are obtained instead at ambient temperatures in buffer. Since this degradation process first requires oxidation of the $[4Fe\text{-}4S]^{2+}$ cluster to the $[4Fe\text{-}4S]^{3+}$ state (eq 1 and 2), the $[3Fe\text{-}4S]^{1+}$ signal indicates, indirectly, oxidation of the cluster.

EPR experiments with AfUDG, furthermore, do show signals characteristic of a $[4Fe\text{-}4S]^{3+}$ cluster in solution when the protein is incubated with DNA and $[Co(phen)_3]^{3+}$, reflecting direct oxidation of the cluster. Interestingly, when this same sample is first heated to 55 °C, the degraded cluster ($[3Fe\text{-}4S]^{1+}$) is observed instead. Oxidation of AfUDG with ferricyanide earlier had shown EPR evidence of both the $[4Fe\text{-}4S]^{3+}$ and $[3Fe\text{-}4S]^{1+}$ clusters (*35*), and here with DNA binding and oxidation with cobalt, a species with *g* values of 2.13 and 2.04, generally characteristic of a $[4Fe\text{-}4S]^{3+}$ cluster (*83*, *84*), is observed. Noteworthy also are fluorescence studies of AfUDG as a function of temperature (*71*) that suggested that, above 50 °C, AfUDG has a more "open" conformation, while the structure is more compact at lower temperature; this also was correlated with the higher activity of the enzyme above 50 °C. It seems that this more open conformation is more susceptible to hydrolytic degradation of the $[4Fe\text{-}4S]^{3+}$ cluster, leading to formation of the $[3Fe\text{-}4S]^{1+}$ cluster (based on the appearance of a species with a *g*-value of 2.01).

It is interesting in this context to consider recent results we have obtained for the DNA-mediated oxidation of MutY by guanine radical (*97*). Oxidized guanine radical in DNA, generated using a flash/quench technique, is found to promote oxidation of the $[4Fe\text{-}4S]^{2+}$ cluster of MutY primarily to $[4Fe\text{-}4S]^{3+}$ along with its decomposition product $[3Fe\text{-}4S]^{1+}$ based upon EPR spectra with *g*-values of 2.08, 2.06, and 2.02. Thus oxidation of the cluster in a rapid DNA-mediated reaction is far more likely to yield $[4Fe\text{-}4S]^{3+}$ with minimum decomposition.

Model for Collaborative Scanning for DNA Lesions by BER Enzymes. While the enzymology of BER enzymes has been increasingly well established, little is understood about how BER repair enzymes first locate their substrates, often single damaged bases in a vast array of undamaged DNA (*1*). The [4Fe-4S] clusters are ubiquitous to these enzymes although a redox function for these clusters had been disregarded early on owing to the lack of redox activity seen with these proteins under physiological conditions (*34*). The data reported here, where DNA binding promotes a shift in redox potential to the physiological range, for all three BER enzymes now require that a redox role for these [4Fe-4S] clusters be revisited.

We propose that the clusters serve as cofactors for DNA-mediated redox signaling among the BER enzymes. Through long-range DNA-mediated charge transport, the BER enzymes may quickly become localized in regions of the genome containing DNA mismatches and lesions. This model is based upon the shift in potential we find for the BER enzymes associated with DNA binding. Thus our proposal reflects the electron exchange reaction among BER enzymes of similar potential bound to DNA as follows:

$$[4Fe\text{-}4S]_A^{2+} + \{DNA-[4Fe\text{-}4S]_B^{3+}\} \leftrightarrow \{DNA-[4Fe\text{-}4S]_A^{3+}\} + [4Fe\text{-}4S]_B^{2+} \quad (3)$$

Figure 8 illustrates this model for this cooperative BER detection strategy. A given BER enzyme, free in solution, contains the [4Fe-4S] cluster in the +2 state, as seen earlier (*34*−*35*, *84*). As such, the protein is robust and insensitive to redox chemistry. As shown here, binding to DNA, however, shifts the redox potential, facilitating oxidation of the [4Fe-4S] cluster to the +3 state. Oxidation, then, can involve a DNA-mediated charge transfer to an alternate BER enzyme bound at a distal site along the DNA with its cluster already in the +3 state. Reduction of this secondary BER enzyme could then facilitate its dissociation from the duplex. This process, as described, in actuality represents a scan of one region of the genome: in the absence of an intervening lesion, mismatch, or other perturbation in base pair stacking, the DNA-mediated charge transfer process can proceed. The similarity in potentials for the different DNA-bound BER enzymes makes such a charge transfer process among DNA-bound $[4Fe\text{-}4S]^{3+/2+}$ clusters near equilibrium plausible; a dynamic equilibrium between oxidized bound enzymes and reduced dissociated enzymes is expected. As also illustrated in Figure 8, the presence of a nearby perturbation in base pair stacking inhibits charge transfer. Under this circumstance, the BER enzyme remains associated with the DNA, allowing DNA-bound facilitated diffusion to the substrate site and repair. This model, then, provides a means to redistribute BER enzymes rapidly away from well-matched DNA and preferentially onto genome sites in the vicinity of DNA lesions.

The results given here provide added support for this model. The shift in redox potential for BER enzymes upon DNA binding is now more widely demonstrated. Additionally, since each BER enzyme is in low copy number within the cell, this model provides a means for the enzymes to cooperate in locating their substrates. Some kinetic evidence for cooperativity in enzyme kinetics had been seen previously (*17*), yet there has been no structural evidence for protein dimerization in the bacterial forms of these enzymes. Our model provides for a cooperativity *among* BER enzymes. Indeed, irrespective of the specific substrate for the BER enzyme, none of the enzymes should populate well-matched, unperturbed regions of the genome; this model provides a mechanism instead for the enzymes to redistribute onto damaged regions of the genome. Thus, by collaborating in their search for DNA damage, the BER enzymes can efficiently locate their substrates.

Implications. The [4Fe-4S] clusters are ubiquitous in BER enzymes, present in homologues from bacteria to man. A clear functional role for these clusters has been lacking, however. Results here provide a basis for establishing a functional role for the [4Fe-4S] clusters of BER enzymes that involves redox chemistry, the common chemistry utilized by most [4Fe-4S] cluster-containing proteins within the cell. The role proposed, moreover, involves DNA-mediated charge transfer chemistry, a reaction that has been amply demonstrated to be sensitive to mismatches, lesions, and other perturbations in base pair stacking. Hence these results provide a framework for reconciling the frequency of [4Fe-4S] clusters in repair enzymes as well as a strategy for

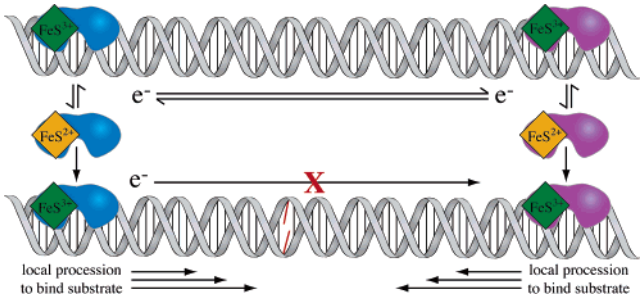

FIGURE 8: Proposed model for long-range DNA signaling between BER enzymes using DNA-mediated charge transfer to detect base lesions. A collaboration among BER enzymes allows for more efficient sorting onto regions of DNA containing base lesions to facilitate substrate detection by these proteins.

effecting the rapid detection of DNA lesions by repair proteins in low copy number. Significantly, these results also provide a basis for considering how the DNA duplex may provide a medium for long-range signaling within the cell.

ACKNOWLEDGMENT

We thank A. Livingston for assistance in preparing enzymes, D. Ceres for technical assistance, and Prof. T. R. O'Connor for generous donation of endonuclease III. We also thank Dr. W. A. Franklin for providing the pET28a-*afung* plasmid and Dr. M. P. Golinelli-Cohen for preparing the pMAL-c2X-*mutY* plasmid.

REFERENCES

1. Lindahl, T. (1993) Instability and decay of the primary structure of DNA, *Nature 362*, 709−715.
2. Friedberg, E. C., Walker, G. C., and Siede, W. (1995) *DNA Repair and Mutagenesis*, ASM Press, Washington, DC.
3. Scharer, O. D. (2003) Chemistry and biology of DNA repair, *Angew. Chem., Int. Ed. Engl. 42*, 2946−2974.
4. David, S. S., and Williams, S. D. (1998) Chemistry of glycosylases and endonucleases involved in base-excision repair, *Chem. Rev. 98*, 1221−1262.
5. Verdine, G. L., and Bruner, S. D. (1997) How do DNA repair proteins locate damaged bases in the genome?, *Chem. Biol. 4*, 329−334.
6. Stivers, J. T., and Jiang, Y. L. (2003) A mechanistic perspective on the chemistry of DNA repair glycosylases, *Chem. Rev. 103*, 2729−2759.
7. Hamilton, R. W., and Lloyd, R. S. (1989) Modulation of the DNA scanning activity of the *Micrococcus luteus* UV endonuclease, *J. Biol. Chem. 264*, 17422−17427.
8. Hildebrandt, E. R., and Cozzarelli, N. R. (1995) Comparison of recombination *in vitro* and in *E. coli* cells: measure of the effective concentration of DNA *in vivo*, *Cell 81*, 331−340.
9. Demple, B., and Harrison, L. (1994) Repair of oxidative damage to DNA: enzymology and biology, *Annu. Rev. Biochem. 63*, 915−948.
10. Bregeon, D., Doddridge, Z. A., You, H. J., Weiss, B., and Doetsch, P. W. (2003) Transcriptional mutagenesis induced by uracil and 8-oxoguanine in *Escherichia coli*, *Mol. Cells 12*, 959−970.
11. Gu, Y., Parker, A., Wilson, T. M., Bai, H., Chang, D. Y., and Lu, A. L. (2002) Human MutY homolog, a DNA glycosylase involved in base excision repair, physically and functionally interacts with mismatch repair proteins human MutS homolog 2/human MutS homolog 6, *J. Biol. Chem. 277*, 11135−11142.
12. Yang, H., Clendenin, W. M., Wong, D., Demple, B., Slupska, M. M., Chiang, J. H., and Miller, J. H. (2001) Enhanced activity of adenine-DNA glycosylase (Myh) by apurinic/apyrimidinic endonuclease (Ape1) in mammalian base excision repair of an A/GO mismatch, *Nucleic Acids Res. 29*, 743−752.
13. Pope, M. A., Porello, S. L., and David, S. S. (2002) *Escherichia coli* apurinic-apyrimidinic endonucleases enhance the turnover of the adenine glycosylase MutY with G:A substrates, *J. Biol. Chem. 277*, 22605−22615.
14. Marenstein, D. R., Ocampo, M. T., Chan, M. K., Altamirano, A., Basu, A. K., Boorstein, R. J., Cunningham, R. P., and Teebor, G. W. (2001) Stimulation of human endonuclease III by Y box-binding protein 1 (DNA-binding protein B). Interaction between a base excision repair enzyme and a transcription factor, *J. Biol. Chem. 276*, 21242−21249.
15. Marenstein, D. R., Chan, M. K., Altamirano, A., Basu, A. K., Boorstein, R. J., Cunningham, R. P., and Teebor, G. W. (2003) Substrate specificity of human endonuclease III (hNTH1). Effect of human APE1 on hNTH1 activity, *J. Biol. Chem. 278*, 9005−9012.
16. Liu, X., Choudhury, S., and Roy, R. (2003) *In vitro* and *in vivo* dimerization of human endonuclease III stimulates its activity, *J. Biol. Chem. 278*, 50061−50069.
17. Wong, I., Bernards, A. S., Miller, J. K., and Wirz, J. A. (2003) A dimeric mechanism for contextual target recognition by MutY glycosylase, *J. Biol. Chem. 278*, 2411−2418.
18. Nunez, M. E., Hall, D. B., and Barton, J. K. (1999) Long-range oxidative damage to DNA: effects of distance and sequence, *Chem. Biol. 6*, 85−97.
19. Kelley, S. O., and Barton, J. K. (1999) Electron transfer between bases in double helical DNA, *Science 283*, 375−381.
20. Kelley, S. O., Holmlin, R. E., Stemp, E. D. A., and Barton, J. K. (1997) Photoinduced electron transfer in ethidium-modified DNA duplexes: dependence on distance and base stacking, *J. Am. Chem. Soc. 119*, 9861−9870.
21. Holmlin, R. E., Dandliker, P. J., and Barton, J. K. (1997) Charge transfer through the DNA base stack, *Angew. Chem., Int. Ed. Engl. 36*, 2715−2730.
22. Schuster, G. B. (2000) Long-range charge transfer in DNA: transient structural distortions control the distance dependence, *Acc. Chem. Res. 33*, 253−260.
23. Giese, B. (2002) Long-distance electron transfer through DNA, *Annu. Rev. Biochem. 71*, 51−70.
24. Bhattacharya, P. K., and Barton, J. K. (2001) Influence of intervening mismatches on long-range guanine oxidation in DNA duplexes, *J. Am. Chem. Soc. 123*, 8649−8656.
25. Hall, D. B., and Barton, J. K. (1997) Sensitivity of DNA-mediated electron transfer to the intervening π-stack: a probe for the integrity of the DNA base stack, *J. Am. Chem. Soc. 119*, 5045−5046.
26. Rajski, S. R., and Barton, J. K. (2001) How different DNA-binding proteins affect long-range oxidative damage to DNA, *Biochemistry 40*, 5556−5564.
27. Boon, E. M., Salas, J. E., and Barton, J. K. (2002) An electrical probe of protein-DNA interactions on DNA-modified surfaces, *Nat. Biotechnol. 20*, 282−286.
28. Boon, E. M., Ceres, D. M., Drummond, T. G., Hill, M. G., and Barton, J. K. (2000) Mutation detection by electrocatalysis at DNA-modified electrodes, *Nat. Biotechnol. 18*, 1096−1100.
29. Nunez, M. E., Noyes, K. T., and Barton, J. K. (2002) Oxidative charge transport through DNA in nucleosome core particles, *Chem. Biol. 9*, 403−415.
30. Nunez, M. E., Holmquist, G. P., and Barton, J. K. (2001) Evidence for charge transport in the nucleus, *Biochemistry 40*, 12465−12471.
31. Friedman, K. A., and Heller, A. (2001) On the non-uniform distribution of guanine in introns of human genes: possible protection of exons against oxidation by proximal intron poly-G sequences, *J. Phys. Chem. B 105*, 11859−11865.
32. Rajski, S. R., Jackson, B. A., and Barton, J. K. (2000) DNA repair: models for damage and mismatch recognition, *Mutat. Res. 447*, 49−72.
33. Boon, E. M., Livingston, A. L., Chmiel, N. H., David, S. S., and Barton, J. K. (2003) DNA-mediated charge transfer for DNA repair, *Proc. Natl. Acad. Sci. U.S.A. 100*, 12543−12547; *101*, 4718.
34. Cunningham, R. P., Asahara, H., Bank, J. F., Scholes, C. P., Salerno, J. C., Surerus, K., Munck, E., McCracken, J., Peisach, J., and Emptage, M. H. (1989) Endonuclease III is an iron−sulfur protein, *Biochemistry 28*, 4450−4455.
35. Hinks, J. A, Evans, M. C. W., de Miguel, Y., Sartori, A. A., Jiricny, J., and Pearl, L. H. (2002) An iron−sulfur cluster in the family 4 uracil-DNA glycosylases, *J. Biol. Chem. 277*, 16936−16940.
36. Rebeil, R., Sun, Y., Chooback, L., Pedraza-Reyes, M., Kinsland, C., Begley, T. P., and Nicholson, W. L. (1998) Spore photoproduct lyase from *Bacillus subtilis* spores is a novel iron−sulfur DNA repair enzyme which shares features with proteins such as class

III anaerobic ribonucleotide reductases and pyruvate-formate lyases, *J. Bacteriol. 180*, 4879−4885.
37. Lee, C. H., Kim, S. H., Choi, J. I., Choi, J. Y., Lee, C. E., and Kim, J. (2002) Electron paramagnetic resonance study reveals a putative iron−sulfur cluster in human rpS3 protein, *Mol. Cells 13*, 154−156.
38. Nghiem, Y., Cabrera, M., Cupples, C. G., and Miller, J. H. (1988) The MutY gene: a mutator locus in *Eshcherichia coli* that generates G:C to T:A transversions, *Proc. Natl. Acad. Sci. U.S.A. 85*, 2709−2713.
39. Michaels, M. L., Cruz, C., Grollman, A. P., and Miller, J. H. (1992) Evidence that MutY and MutM combine to prevent mutations by an oxidatively damaged form of guanine in DNA, *Proc. Natl. Acad. Sci. U.S.A. 89*, 7022−7025.
40. Michaels, M. L., and Miller, J. H. (1992) The GO system protects organisms from the mutagenic effect of the spontaneous lesion 8-hydroxyguanine (7,8-dihydro-8-oxoguanine), *J. Bacteriol. 174*, 6321−6325.
41. Michaels, M. L., Tchou, J., Grollman, A. P., and Miller, J. H. (1992) A repair system for 8-oxo-7,8-dihydrodeoxyguanine, *Biochemistry 17*, 10964−10968.
42. Gogos, A., Cillo, J., Clarke, N. D., and Lu, A. L. (1996) Specific recognition of A/G and A/7,8-dihydro-8-oxoguanine (8-oxoG) mismatches by *Escherichia coli* MutY: removal of the C-terminal domain preferentially affects A/8-oxoG recognition, *Biochemistry 35*, 16665−16671.
43. Lu, A. L., Tsai-Wu, J. J., and Cillo, J. (1995) DNA determinants and substrate specificities of *Escherichia coli* MutY, *J. Biol. Chem. 270*, 23582−23588.
44. Manuel, R. C., Czerwinski, E. W., and Lloyd, R. S. (1996) Identification of the structural and functional domains of MutY, an *Escherichia coli* DNA mismatch repair enzyme, *J. Biol. Chem. 271*, 16218−16226.
45. Manuel, R. C., and Lloyd, R. S. (1997) Cloning, overexpression, and biochemical characterization of the catalytic domain of MutY, *Biochemistry 36*, 11140−11152.
46. Francis, A. W., Helquist, S. A., Kool, E. T., and David, S. S. (2003) Probing the requirements for recognition and catalysis in Fpg and MutY with nonpolar adenine isosteres, *J. Am. Chem. Soc. 125*, 16235−16242.
47. Chepanoske, C. L., Porello, S. L., Fujiwara, T., Sugiyama, H., and David, S. S. (1999) Substrate recognition by *Escherichia coli* MutY using substrate analogs, *Nucleic Acids Res. 27*, 3197−3204.
48. Vidmar, J. J., and Cupples, C. G. (1993) MutY repair is mutagenic in MutT-strains of *Escherichia coli*, *Can. J. Microbiol. 39*, 892−894.
49. Bulychev, N. V., Varaprasad, C. V., Dorman, G., Miller, J. H., Eisenberg, M., Grollman, A. P., and Johnson, F. (1996) Substrate specificity of *Escherichia coli* MutY protein, *Biochemistry 35*, 13147−13156.
50. Porello, S. L., Leyes, A. E., and David, S. S. (1998) Single-turnover and pre-steady-state kinetics of the reaction of the adenine glycosylase MutY with mismatch-containing DNA substrates, *Biochemistry 37*, 14756−14764.
51. Radicella, J. P., Clark, E. A., and Fox, M. S. (1988) Some mismatch repair activities in *Escherichia coli*, *Proc. Natl. Acad. Sci. U.S.A. 95*, 9674−9678.
52. Guan, Y., Manuel, R. C., Arvai, A. S., Parikh, S. S., Mol, C. D., Miller, J. H., Lloyd, S., and Tainer, J. A. (1998) MutY catalytic core, mutant and bound adenine structures define specificity for DNA repair enzyme superfamily, *Nat. Struct. Biol. 5*, 1058−1064.
53. Michaels, M. L., Pham, L., Nghiem, Y., Cruz, C., and Miller, J. H. (1990) MutY, an adenine glycosylase active on G-A mispairs, has homology to endonuclease III, *Nucleic Acids Res. 18*, 3841−3845.
54. Demple, B., and Linn, S. (1980) DNA N-glycosylases and UV repair, *Nature 287*, 203−208.
55. Katcher, H. L., and Wallace, S. S. (1983) Characterization of the *Escherichia coli* X-ray endonuclease, endonuclease III, *Biochemistry 22*, 4071−4081.
56. Breimer, L. H., and Lindahl, T. (1984) DNA glycosylase activities for thymine residues damaged by ring saturation, fragmentation, or ring contraction are functions of endonuclease III in *Escherichia coli*, *J. Biol. Chem. 259*, 5543−5548.
57. Duker, N. J., and Weiss, R. B. (1986) Photoalkylated DNA and ultraviolet-irradiated DNA are incised at cytosines by endonuclease III, *Nucleic Acids Res. 26*, 6621−6631.
58. Boorstein, R. J., Hilbert, T. P., Cadet, J., Cunningham, R. P., and Teebor, G. W. (1989) UV-induced pyrimidine hydrates in DNA are repaired by bacterial and mammalian DNA glycosylase activities, *Biochemistry 28*, 6164−6170.
59. Wagner, J. R., Blount, B. C., and Weinfeld, M. (1996) Excision of oxidative cytosine modifications from gamma-irradiated DNA by *Escherichia coli* endonuclease III and human whole-cell extracts, *Anal. Biochem. 233*, 76−86.
60. Dizdaroglu, M., Laval, J., and Boiteux, S. (1993) Substrate specificity of the *Escherichia coli* endonuclease III: excision of thymine- and cytosine-derived lesions in DNA produced by radiation-generated free radicals, *Biochemistry 32*, 12105−12111.
61. Kuo, C. F., McRee, D. E., Fisher, C. L., O'Handley, S. F., Cunningham, R. P., and Tainer, J. A. (1992) Atomic structure of the DNA repair [4Fe-4S] enzyme endonuclease III, *Science 258*, 434−440.
62. Thayer, M. M., Ahern, H., Xing, D., Cunningham, R. P., and Tainer, J. A. (1995) Novel DNA binding motifs in the DNA repair enzyme endonuclease III crystal structure, *EMBO J. 14*, 4108−4120.
63. Cowan, J. A., and Lui, S. M. (1998) Structure−function correlations in high-potential iron proteins, *Adv. Inorg. Chem. 45*, 313−350.
64. Fu, W., O'Handley, S., Cunningham, R. P., and Johnson, M. K. (1992) The role of the iron−sulfur cluster in *Escherichia coli* endonuclease III. A resonance Raman study, *J. Biol. Chem. 267*, 16135−16137.
65. Porello, S. L., Cannon, M. J., and David, S. S. (1998) A substrate recognition role for the $[4Fe\text{-}4S]^{2+}$ cluster of the DNA repair glycosylase MutY, *Biochemistry 37*, 6465−6475.
66. Lu, A. L., and Fawcett, W. P. (1998) Characterization of the recombinant MutY homolog, an adenine DNA glycosylase, from yeast *Schizosaccharomyces pombe*, *J. Biol. Chem. 273*, 25098−25105.
67. McGoldrick, J. P., Yeh, Y. C., Solomon, M., Essigmann, J. M., and Lu, A. L. (1995) Characterization of a mammalian homolog of the *Escherichia coli* MutY mismatch repair protein, *Mol. Cell. Biol. 15*, 989−996.
68. Ikeda, S., Biswas, T., Roy, R., Izumi, T., Boldogh, I., Kurosky, A., Sarker, A. H., Seki, S., and Mitra, S. (1998) Purification and characterization of human NTH1, a homolog of *Escherichia coli* endonuclease III. Direct identification of Lys-212 as the active nucleophilic residue, *J. Biol. Chem. 273*, 21585−21593.
69. Pearl, L. H. (2000) Structure and function in the uracil-DNA glycosylase superfamily, *Mutat. Res. 460*, 165−181.
70. Hoseki, J., Okamoto, A., Masui, R., Shibata, T., Inoue, Y., Yokoyama, S., and Kuramitsu, S. (2003) Crystal structure of a family 4 uracil-DNA glycosylase from *Thermus thermophilus* HB8, *J. Mol. Biol. 333*, 515−526.
71. Knaevlsrud, I., Ruoff, P., Anensen, H., Klungland, A., Bjelland, S., and Birkeland, N. K. (2001) Excision of uracil from DNA by the hyperthermophilic Afung protein is dependent on the opposite base and stimulated by heat-induced transition of a more open structure, *Mutat. Res. 487*, 173−190.
72. Sartori, A. A., Schar, P., Fitz-Gibbon, S., Miller, J. H., and Jiricny, J. (2001) Biochemical characterization of uracil processing activities in the hyperthermophilic archaeon *Pyrobaculum aerophilum*, *J. Biol. Chem. 276*, 29979−29986.
73. Sandigursky, M., Faje, A., and Franklin, W. A. (2001) Characterization of the full length uracil-DNA glycosylase in the extreme thermophile *Thermotoga maritima*, *Mutat. Res. 485*, 187−195.
74. Sandigursky, M., and Franklin, W. A. (2000) Uracil-DNA glycosylase in the extreme thermophile *Archaeoglobus fulgidus*, *J. Biol. Chem. 275*, 19146−19149.
75. Lindahl, T., and Nyberg, B. (1974) Heat-induced deamination of cytosine residues in deoxyribonucleic acid, *Biochemistry 13*, 3405−3410.
76. Jacobs, K. L., and Grogan, D. W. (1997) Rates of spontaneous mutation in an archaeon from geothermal environments, *J. Bacteriol. 179*, 3298−3303.
77. Thomas, N. C., Pringle, K., and Deacon, G. B. (1989) Cobalt(II) and cobalt(III) coordination compounds, *J. Chem. Educ. 66*, 516−517.
78. Asahara, H., Wistort, P. M., Bank, J. F., Bakerian, R. H., and Cunningham, R. P. (1989) Purification and characterization of *Escherichia coli* endonuclease III from the cloned nth gene, *Biochemistry 28*, 4444−4449.
79. Beaucage, S. L., and Caruthers, M. H. (1981) Dexoynucleoside phosphoramidites—a new class of key intermediates for deoxypolynucleotide synthesis, *Tetrahedron Lett. 22*, 1859−1862.

80. Kelley, S. O., Boon, E. M., Barton, J. K., Jackson, N. M., and Hill, M. G. (1999) Single-base mismatch detection based on charge transduction through DNA, *Nucleic Acids Res. 27*, 4830−4837.
81. Tender, L., Carter, M. T., and Murray, R. W. (1994) Cyclic voltammetric analysis of ferrocene alkanethiol monolayer electrode kinetics based on Marcus theory, *Anal. Chem. 66*, 3173−3181.
82. Armstrong, F. A., Heering, H. A., and Hirst, J. (1997) Reactions of complex metalloproteins studied by protein-film voltammetry, *Chem. Soc. Rev. 26*, 169−188.
83. Guo, L. H., and Hill, H. A. O. (1991) Direct electrochemistry of proteins and enzymes, *Adv. Inorg. Chem. 36*, 341−375.
84. Lukianova, O. A., and David, S. S. (2005) A role for iron-sulfur clusters in DNA repair, *Curr. Opin. Chem. Biol. 9*, 145−151.
85. Camba, R., and Armstrong, F. A. (2000) Investigations of the oxidative disassembly of Fe-S clusters in *Clostridium pasteurianum* 8Fe ferredoxin using pulsed-protein-film voltammetry, *Biochemistry 39*, 10587−10598.
86. Roth, E. K. H., and Jordanov, J. (1991) Oxidation reactions of $[Fe_4S_4(S\text{-}2,4,6\text{-}(iso\text{-}Pr)_3C_6H_2)_4]^{2-}$ and an oxidative conversion of the Fe_4S_4 core into an Fe_3S_4 center, *Inorg. Chem. 30*, 240−243.
87. Dilg, A. W. E., Mincione, G., Acterhold, K., Iakovleva, O., Mentler, M., Luchinat, C., Bertini, I., and Parak, F. G. (1999) Simultaneous interpretation of Mossbauer, EPR, and ^{57}Fe ENDOR spectra of the [Fe4S4] cluster in the high-potential iron protein I from *Ectothiorhodospira halophila*, *J. Biol. Inorg. Chem. 4*, 727−741.
88. Heering, H. A., Bulsink, Y. B. M., Hagen, W. R., and Meyer, T. E. (1995) Reversible super-reduction of the cubane [4Fe-4S]$^{(3+;2+;1+)}$ in the high-potential iron−sulfur protein under non-denaturing conditions, *Eur. J. Biochem. 232*, 811−817.
89. Huynh, B. H., Moura, J. J. G., Moura, I., Kent, T. A., Legall, J., Xavier, A. V., and Munck, E. (1980) Mossbauer and EPR studies of desulforedoxin from *Desulfovibrio gigas*, *J. Biol. Chem. 255*, 3242−3244.
90. Ruzicka, F. J., and Beinert, J. (1978) The soluble "high potential" type iron−sulfur protein from mitochondria is aconitase, *J. Biol. Chem. 253*, 2514−2517.
91. Carter, M. T., Rodriguez, M., and Bard, A. J. (1989) Voltammetric studies of the interaction of metal chelates with DNA. 2. Tris-chelated complexes of cobalt(III) and iron(II) with 1, 10-phenanthroline and 2, 2′-bipyridine, *J. Am. Chem. Soc. 111*, 8901−8911.
92. Rehmann, J. P., and Barton, J. K. (1990) ^{1}H NMR studies of tris-(phenanthroline) metal complexes bound to oligonucleotides: characterization of binding modes, *Biochemistry 29*, 1701−1709.
93. Sticht, H. and Rosch, P. (1998) The structure of iron−sulfur proteins, *Prog. Biophys. Mol. Biol. 70*, 95−136.
94. Fromme, J. C., Banerjee, A., Huang, S. J., and Verdine, G. L (2004) Structural basis for removal of adenine mispaired with 8-oxoguanine by MutY adenine DNA glycosylase, *Nature 427*, 652−656.
95. Fromme, J. C., and Verdine, G. L (2003) Structure of a trapped endonuclease III-DNA covalent intermediate, *EMBO J. 22*, 3461−3471.
96. Carter, C. W., Kraut, J., Freer, S. T., Alden, R. A., Sieker, L. C., Adman, E. and Jensen, L. H. (1972) A comparison of Fe4S4 clusters in high potential iron protein and in ferredoxin, *Proc. Natl. Acad. Sci. U.S.A. 69*, 3526−3529.
97. Yavin, E., Boal, A. K., Stemp, E. D. A., Boon, E. M., Livingston, A. L., O'Shea, V. L., David, S. S., and Barton, J. K. (2005) Protein-DNA Charge Transport: Redox Activation of a DNA Repair Protein by Guanine Radical, *Proc. Natl. Acad. Sci. U.S.A. 102*, 3546−3551.

BI047494N